TABLE 1. PLASMA RALTEGRAVIR CONCENTRATIONS AND PATIENT CHARACTERISTICS FOR EACH *UGT1A1* GENOTYPE IN 56 PATIENTS

	Wild-type	*Heterozygote*	*Homozygote*	p *value*
*6 genotypes				
n	41	13	2	
Male:female	37:4	12:1	1:1	n.s.
Age (years) (mean±SD)	50±15	50±11	41 and 69	0.807
Weight (kg) (mean±SD)	62.3±11.0	68.3±7.6	43.9 and 33.9	0.005
Raltegravir concentration (μg/ml) (mean±SD)	0.12±0.09	0.16±0.10	0.53 and 0.03	0.230
*28 genotypes				
n	45	11	0	
Male:female	40:5	10:1	—	n.s.
Age (years) (mean±SD)	49±13	52±18	—	0.606
Weight (kg) (mean±SD)	63.7±12.3	59.2±5.9	—	0.078
Raltegravir concentration (μg/ml) (mean±SD)	0.14±0.11	0.11±0.09	—	0.502

n.s., not significant ($p>0.05$). All of the patients were found to be wild type for the *27 allele (i.e., *27−/−).

regimen. On the other hand, patients heterozygous for the *6 or *28 allele did not display significantly different plasma raltegravir concentrations when compared to patients homozygous for the respective wild-type allele (Fig. 1A and B).

Table 1 shows plasma raltegravir concentrations and patient characteristics sorted by the *UGT1A1* genotype of the 56 patients. The body weights of the two patients with the *6 homozygote were lower than those of patients who were wild type or heterozygous for this allele, and this difference was statistically significant. However, the other differences in patient characteristics for each *UGT1A1* genotype (*6 and *28) were not significant, indicating that these characteristics did not correlate with the differences in raltegravir concentration seen among *UGT1A1* genotypes.

Table 2 shows the relationship between *UGT1A1* genotype (both *6 and *28) and raltegravir concentration in the 56 patients. Plasma raltegravir concentrations were 0.12 μg/ml (*6−/− *28−/−; $n=30$), 0.11 μg/ml (*6−/− *28−/+; $n=11$), and 0.16 μg/ml (*6−/+ *28−/−; $n=13$). There were no statistically significant differences in the plasma raltegravir concentrations between patients carrying wild-type alleles and those heterozygous for *6 or *28.

Discussion

The polymorphisms (*6, *27, and *28 alleles) associated with the *UGT1A1* locus lead to deficiencies in UGT1A1 activity. As a result, individuals with these alleles may have higher plasma raltegravir concentrations. In fact, Wenning *et al.*[11] reported that plasma raltegravir concentrations are modestly higher in individuals with the *UGT1A1*28* homozygote compared to those carrying the wild-type allele. Regrettably, we could not confirm this result because we identified no patients with the *28 homozygote among our 56 recruited patients. Within our patient sample, there were no statistically significant differences in plasma raltegravir concentrations between patients with wild-type and *28 heterozygous genotypes. Further assessment of the relationship between the *UGT1A1*28* genotype and plasma raltegravir concentrations will require studies on additional subjects.

TABLE 2. RELATIONSHIP BETWEEN *UGT1A1* GENOTYPE (*6 AND *28) AND RALTEGRAVIR CONCENTRATION IN 56 PATIENTS

6 genotype	*28 genotype*	n	*Raltegravir concentration (μg/ml) (mean±SD)*	p *value*
−/−	−/−	30	0.12±0.09	—
−/−	−/*28	11	0.11±0.09	0.848
−/*6	−/−	13	0.16±0.10	0.106
*6/*6	−/−	2	0.53 and 0.03	0.725

The *UGT1A1*6* and *27 polymorphisms are commonly found among Asians, where the *UGT1A1*6* polymorphism is more common than *UGT1A1*28*.[8] Among our 56 recruited patients, we found 2 patients with the *6 homozygote and another 13 patients with the *6 heterozygote. On the other hand, all 56 of our patients carried wild-type sequences at the position corresponding to the *27 allele. In the single male patient homozygous for *6, the plasma raltegravir concentration (0.53 μg/ml) was modestly higher than that seen in patients with wild-type alleles (0.12 μg/ml) or *6 heterozygosity (0.16 μg/ml). The single female patient homozygous for *6 had a lower plasma raltegravir concentration (0.03 μg/ml). Thus, in this study, we examined only a small number of patients with the *6 homozygote. In addition, the intraindividual variability in raltegravir concentration is known to be very large.[12] As a result of these limitations, we could not demonstrate any correlation between *UGT1A1*6* homozygosity and plasma raltegravir concentration. This observation is similar to that of Neely *et al.*[13] who reported that the high degree of variability in raltegravir concentration and small population size appeared to obscure any pharmacogenomic effects on plasma raltegravir concentrations by the *28 allele.

Our results also indicated that heterozygosity for the reduced-function *6 and *28 alleles appeared to have no significant effect on plasma raltegravir concentrations in Japanese HIV-1-infected patients. Additional clarification of the contribution of the *UGT1A1* *6 and *28 polymorphisms to plasma raltegravir concentrations will require further investigations with larger subject populations.

Acknowledgments

This study was supported in part by a Grant-in-Aid for Clinical Research from the National Hospital Organization to M.T.

Author Disclosure Statement

No competing financial interests exist.

References

1. Hazuda DJ, Felock P, Witmer M, Wolfe A, Stillmock K, Grobler JA, Espeseth A, Gabryelski L, Schleif W, Blau C, and Miller MD: Inhibitors of strand transfer that prevent integration and inhibit HIV-1 replication in cells. Science 2000;287:646–650.
2. Cahn P and Sued O: Raltegravir: A new antiretroviral class for salvage therapy. Lancet 2007;369:1235–1236.
3. Croxtall JD, Lyseng-Williamson KA, and Perry CM: Raltegravir. Drugs 2008;68:131–138.
4. Evering TH and Markowitz M: Raltegravir (MK-0518): An integrase inhibitor for the treatment of HIV-1. Drugs Today (Barc) 2007;43:865–877.
5. Department of Health and Human Services: Panel on Antiretroviral Guidelines for Adults and Adolescents: Guidelines for the use of antiretroviral agents in HIV-1-infected adults and adolescents. 2011;1–166. Available at http://www.aidsinfo.nih.gov/ContentFiles/AdultandAdolescentGL.pdf. Accessed September 1, 2011.
6. Pharmacogenomics Laboratory: Canada Research Chair in Pharmacogenomics www.pharmacogenomics.pha.ulaval.ca/sgc/.
7. Huang YY, Huang MJ, Yang SS, Teng HC, and Huang CS: Variations in the UDP-glucuronosyltransferase 1A1 gene for the development of unconjugated hyperbilirubinemia in Taiwanese. Pharmacogenomics 2008;9:1229–1235.
8. Palomaki GE, Bradley LA, Douglas MP, Kolor K, and Dotson WD: Can UGT1A1 genotyping reduce morbidity and mortality in patients with metastatic colorectal cancer treated with irinotecan? An evidence-based review. Genet Med 2009;11:21–34.
9. Ehmer U, Lankisch TO, Erichsen TJ, Kalthoff S, Freiberg N, Wehmeier M, Manns MP, and Strassburg CP: Rapid allelic discrimination by TaqMan PCR for the detection of the Gilbert's syndrome marker UGT1A1*28. J Mol Diagn 2008;10:549–552.
10. Takahashi M, Konishi M, Kudaka Y, Okumura N, Hirano A, Terahata N, Banno K, and Kaneda T: A conventional LC-MS method developed for the determination of plasma raltegravir concentrations. Biol Pharm Bull 2008;31:1601–1604.
11. Wenning LA, Petry AS, Kost JT, Jin B, Breidinger SA, DeLepeleire I, Carlini EJ, Young S, Rushmore T, Wagner F, Lunde NM, Bieberdori F, Greenberg H, Stone JA, Wagner JA, and Iwamoto M: Pharmacokinetics of raltegravir in individuals with UGT1A1 polymorphisms. Clin Pharmacol Ther 2009;85:623–627.
12. Anderson MS, Kakuda TN, Hanley W, Miller J, Kost JT, Stoltz R, Wenning LA, Stone JA, Hoetelmans RMW, Wagner JA, and Iwamoto M: Minimal pharmacokinetic interaction between the human immunodeficiency virus nonnucleoside reverse transcriptase inhibitor etravirine and the integrase inhibitor raltegravir in healthy subjects. Antimicrob Agents Chemother 2008;52:4228–4232.
13. Neely M, Decosterd L, Fayet A, Lee JS, Margol A, Kanani M, di Iulio J, von Schoen-Angerer T, Jelliffe R, and Calmy A: Pharmacokinetics and pharmacogenomics of once-daily raltegravir and atazanavir in healthy volunteers. Antimicrob Agents Chemother 2010;54:4619–4625.

Address correspondence to:
Masaaki Takahashi
Department of Pharmacy
National Hospital Organization Nagoya Medical Center
Sannomaru 4-1-1, Naka-ku, Nagoya
Aichi 460-0001
Japan

E-mail: masaakit@nnh.hosp.go.jp

日消誌　2012；109：1186―1196

原　著

当院におけるHIV，HCV重複感染症例に対するペグインターフェロン，リバビリン併用療法の治療成績

都築智之　岩瀬弘明　島田昌明[1)]
平嶋昇[2)]　日比野祐介　龍華庸光
齋藤雅之　玉置大　神谷麻子
横井美咲[1)]　横幕能行[3)]　藤崎誠一郎[4)]
杉浦亙[5)]　後藤秀実[6)]

要旨：名古屋医療センターにてHIV，HCV重複感染10症例に対しペグインターフェロン，リバビリン併用療法が行われた．HCV genotypeは，1bが3例，3bが2例，2b，2c，3a，4a，6nがそれぞれ1例ずつであった．9例に抗HIV療法が併用され，そのうち5例で抗HIV剤の変更が行われた．予定治療完遂例は7例であった．全例で治療中に重篤な有害事象は認めなかった．HCVの持続的ウイルス陰性化は，genotype　1または4で4例中1例（25%），1または4以外で6例中5例（83%）に認められた．HIV，HCV重複感染症例に対する本治療法は，安全で有用な治療と考えられた．

索引用語：C型慢性肝炎，HIV，ペグインターフェロン，リバビリン，HCV genotype

背　景

近年，本邦におけるヒト免疫不全ウイルス（human immunodeficiency virus；HIV）感染者は増加の傾向にある．一般に血液媒介感染であるHIV感染はC型肝炎ウイルス（hepatitis C virus；HCV）重複感染を合併する頻度が高く，本邦のHIV感染者の約2割弱がHCV感染者と推測されており[1)]，中でもHIV陽性の血友病患者におけるHCV感染は約98%と報告されている[2)]．また，近年の抗HIV療法の進歩にともない日和見感染は減少し，HCVにより予後が決定される頻度が増加している．わが国での調査では，1997年から2006年におけるHIV，HCV重複感染のある血液凝固疾患症例の死因は，43%がHCVによるものと報告されており，HIV感染者の診療におけるC型慢性肝炎の治療は大きな課題となっている[2)]．

I　目　的

HIV，HCV重複感染例におけるペグインターフェロン（PEG-IFN），リバビリン（RBV）併用療法は，HCV単独感染に対する治療の場合とは異なった問題点がいくつか存在する．まず，HIV

1）国立病院機構名古屋医療センター消化器科
2）国立病院機構東名古屋病院消化器科
3）国立病院機構名古屋医療センター感染症科
4）国立感染症研究所インフルエンザウイルス研究センター
5）国立病院機構名古屋医療センター臨床研究センター
6）名古屋大学大学院医学系研究科消化器内科学
Corresponding author：都築　智之（tsuzukit@nnh.hosp.go.jp）

感染症に対する多剤併用抗ウイルス療法（highly active anti-retroviral therapy；HAART）は，CD4陽性細胞数を維持することでより安全にPEG-IFN，RBV併用療法を可能とする反面，薬物相互作用による有害事象により治療薬の減量につながることもあり，治療成績の低下の一因ともなり得る[3)4)]．また，C型慢性肝炎のウイルス側の因子としてHCV genotypeはPEG-IFN，RBV併用療法の治療成績に大きく関わる因子と考えられているが，その感染経路が単独感染とは若干異なるHIV重複感染者において，1b，2a，2b以外の国内におけるHCV単独症例ではまれなgenotypeもある程度の頻度で存在しており，それらの症例の治療成績に関するわが国での報告は少ない．以上のことをふまえて，厚生労働省指定エイズ対策東海ブロック拠点病院である名古屋医療センターにおける同治療の現状を検討し，その問題点を明らかにすることを目的とした．

II 対象と方法

2004年12月から2011年4月までに当院でPEG-IFN，RBV併用療法を行ったHIV，HCV重複感染例全症例を対象に，患者背景，HCV genotype，治療成績，副作用を検討した．投与薬剤のadherenceは，投与期間中の予定投与量に対する総投与量の割合と定義し，症例ごとに検討した．HCV genotypeは，C/E1およびNS5B領域の塩基配列に基づいて分類した．リファレンスの配列は，Los Alamos研究所のHCV sequence databaseから取得し，系統樹作成は，maximum likelihood法にてreplication 1000回の条件で行った[5)6)]．

治療における薬剤選択と投与量は，HCV単独感染に対する治療に準じて行われたが，全例PEG-IFNα2bが用いられた．投与期間は，genotype 1または4では48～72週，genotype 1または4以外では24～48週を目標とし，genotype，副作用および治療反応性に応じて決定した．

また，対象患者の母集団である，同時期に当院で診療したHIV陽性患者でHCV-RNA陽性が判明している29例のうち，PEG-IFN，RBV併用療法の対象と考えられた27例のHCV genotypeについても検討した．

III 結 果

対象症例の背景因子と治療結果をTable 1に示す．対象症例は10例，男性7例，女性3例，平均年齢は40.5±12.7歳で，女性は3例とも40歳未満であった．人種は，黄色人種が8例，白色人種が2例（症例3，7）であった．推測感染地域は，国内が5例と半数にとどまっており，そのうちの2例（症例1，6）は血友病に対する輸入非加熱血液製剤が感染源と考えられた．表には示さなかったが，感染経路は先述の2例が輸入非加熱血液製剤，4例が男性同性愛，2例が経静脈麻薬常習，2例が不明であった．HCV genotypeは，1bが3例，3bが2例，2b，2c，3a，4a，6nがそれぞれ1例ずつであった．ウイルス量は全例5 logIU/m*l*以上であった．C型慢性肝炎の推測罹病期間は平均9.9±2.3年で，6例において10年以内と比較的短かった．習慣飲酒者は3例で，飲酒量は20～40g/日であった．なお表には示さなかったが，全例においてHBs抗原は陰性であった．治療前検査結果の平均値はそれぞれ，ALT 83±55IU/*l*，白血球6700±1600/μ*l*，ヘモグロビン14.3±1.8g/d*l*，血小板20.2±5.9×10^4/μ*l*であった．肝生検については2例で施行されており，いずれもF2以下であった．

治療期間は，治療反応性不良や副作用にて治療中断となった3症例を含め，最短で12週，最長で48週であった．genotype 1または4の症例では4例中2例（50%）において48週投与が行われ，1例では治療反応性不良にて32週で，1例ではインフルエンザ様症状の副作用にて24週で中止となった．genotype 1または4以外の6例においては，3例（50%）で48週，2例（33%）で24週の投与が行われ，1例で治療反応性不良にて12週で中止となった．治療成績は，全体でみると持続的ウイルス陰性化（SVR）を6例（60%）に認めた．genotype 1または4高ウイルス症例においてSVRは4例中1例（25%），無効1例，治療中の再燃（breakthrough）1例，治療後の再燃1例であった．genotype 1または4以外の症例では，SVRを6例のうち5例（83%）に認め，

Table 1. 患者背景とPEG-IFN/RBV併用療法の効果

症例	性	年齢	人種	HCV genotype	HCV-RNA (logIU/ml)	HCV推測感染地域	HCVの罹病期間(年)	飲酒量(g/日)	ALT (IU/l)	T-Bil (mg/dl)	Alb (g/dl)	WBC (/μl)	Hb (g/dl)	Plt (×10⁴/μl)	肝生検	adherence (%) PEG-IFN	adherence (%) RBV	副作用	HCV-RNA陰性化時期(週)	治療期間(週)	治療効果
1	M	30歳代	黄色	1b	6.0	国内*	25	20	38	0.91	4.4	8100	16.4	24.2	未検	100	100		陰性化せず	48	NR
2	M	40歳代	黄色	1b	6.0	国内	2	0	78	1.03	4.5	6700	15.1	23.9	未検	100	100		4	48	SVR
3	F	20歳代	白色	1b	6.1	ヨーロッパ	7	0	136	0.76	3.3	4600	12.4	11.8	未検	50	100	抑鬱	8	32	BT
4	M	60歳代	黄色	2b	6.4	国内	20	0	31	1.35	4.4	8800	12.4	12.5	未検	70	65	WBC, Hb減少	8	48	SVR
5	M	30歳代	黄色	2c	7.0	国内	10	30	69	0.40	5.0	6000	14.9	28.3	A2F1	100	100		8	24	SVR
6	M	40歳代	黄色	3a	5.9	国内*	30	0	78	1.58	3.8	6800	13.1	16.3	未検	70	70	WBC, Plt, Hb減少	8	48	SVR
7	M	30歳代	白色	3b	6.3	南アジア	4	40	94	0.68	4.7	6300	16.1	18.6	A2F2	100	100		4	24	SVR
8	F	30歳代	黄色	3b	6.8	東アジア	3	0	28	0.51	4.4	4900	12.9	18.0	未検	50	100	WBC減少	陰性化せず	12	NR
9	F	30歳代	黄色	4a	5.8	東南アジア	9	0	66	0.55	4.2	5200	12.8	19.6	未検	100	100	インフルエンザ様症状	16	24	Rel
10	M	50歳代	黄色	6n	6.7	東南アジア	13	0	212	0.65	5.0	9400	17.3	28.7	未検	100	100		8	48	SVR

*；国内での輸入非加熱血液製剤による感染，PEG-IFN；ペグインターフェロン，RBV；リバビリン，adherence；総投与量/投与期間中の予定投与量，NR；non-response，SVR；sustained virological response，BT；virological breakthrough，Rel；relapse.

Table 2. HIV治療の状況

症例	IFN前CD4陽性細胞数(/μl)	IFN投与中のCD4陽性細胞数最少値(/μl)	IFN前HIV-1定量(copies/ml)	IFN投与中のHIV-1定量最高値(copies/ml)	HIV治療(HAART)	HIV治療の変更	HIV治療の変更時期
1	631	455	1.0×10^5	1.0×10^5	なし		
2	599	344	検出せず	検出せず	AZT, 3TC, NVP	ABC, 3TC, NVP	IFN導入12週前
3	599	393	検出せず	2.0×10^4	TDF, FTC, EFV		
4	488	111	検出せず	検出せず	ABC, 3TC, LPV/r		
5	532	416	検出せず	検出せず	AZT, 3TC, EFV	TDF, FTC, RAL	IFN導入時
6	461	116	検出せず	検出せず	AZT, 3TC, LPV/r	TDF, 3TC, LPV/r	IFN導入2週後
7	590	344	検出せず	検出せず	TDF, FTC, EFV	TDF, FTC, RAL	IFN導入24週前
8	711	533	検出せず	検出せず	TDF, FTC, FPV		
9	323	119	検出せず	検出せず	AZT, 3TC, SQV-HGC, RTV	ABC, 3TC, SQV-HGC, RTV	IFN導入6週前
10	935	490	検出せず	検出せず	d4T, 3TC, NVP		

AZT：ジドブジン，3TC：ラミブジン，NVP：ネビラピン，ABC：アバカビル，TDF：テノホビル，FTC：エムトリシタビン，EFV：エファビレンツ，LPV/r：ロピナビル（少量リトナビル含有），RAL：ラルテグラビル，FPV：ホスアンプレナビル，SQV-HGC：サキナビル，RTV：リトナビル，d4T：サニルブジン．

無効1例であった．

PEG-IFN，RBV併用療法中の血球減少に対して4例でPEG-IFNの減量を，2例でRBVの減量が必要であった．PEG-IFNのadherenceは最低で50%，RBVのadherenceは最低で65%であった．治療経過全般を通じて全例において重篤な副作用は認めなかった．

Table 2にHIVに対する治療について示した．PEG-IFN，RBV併用療法開始前のCD4陽性細胞数は323～935/μlであったが，併用療法中の白血球の減少にともない全例でその減少を認めた．日和見感染症を発症しやすいとされるCD4陽性細胞数200/μl以下への減少は3例に認めたが，全症例において治療中に日和見感染症の合併は認めていない．PEG-IFN, RBV併用療法開始前のHIV-1定量値は，1例（症例1）で1.0×10^5copies/mlであったが，この症例は経過観察のみでCD4陽性細胞数が500/μl以上を維持していた．HAARTについては，この1例を除いて9例にPEG-IFN，RBV併用療法開始前から行われていた．そのうち，1例（症例4）はIFN治療を開始することを前提に開始24週前にHAARTが開始されており，その他の症例は以前よりHAARTが行われていた．PEG-IFN，RBV併用療法の開始に当たって，4例がジドブジン（AZT）から他の核酸系逆転写酵素阻害剤に変更が行われた．変更時期については1例（症例6）でPEG-IFN，RBV併用療法開始2週後，1例（症例5）で同併用療法開始とほぼ同時期に，他の3例（症例2，7，9）は同併用療法の開始6～24週前に変更されていた．PEG-IFN，RBV併用療法開始2週後にAZTを変更した症例は消化器科と感染症科の連絡不行き届きで，AZTを変更する前にPEG-IFN，RBV併用療法が開始されたことにより，急速に貧血を呈し，一時PEG-IFN，RBV併用療法が中止となった．その後AZTをテノホビル(TDF)に変更し，速やかに貧血は改善しPEG-IFN，RBV併用療法の再開が可能となり，その後も貧血，好中球減少，CD4陽性細胞数減少を認めたが48週間の投与を行うことができた（Figure 1）．また，非核酸系逆転写酵素阻害剤のエファビレンツ（EFV）は抑鬱などの精神症状をきたしやすいことを理由に，PEG-IFN，RBV併用療法導入に当たって2症例（症例5，7）において他の薬剤に変更が行

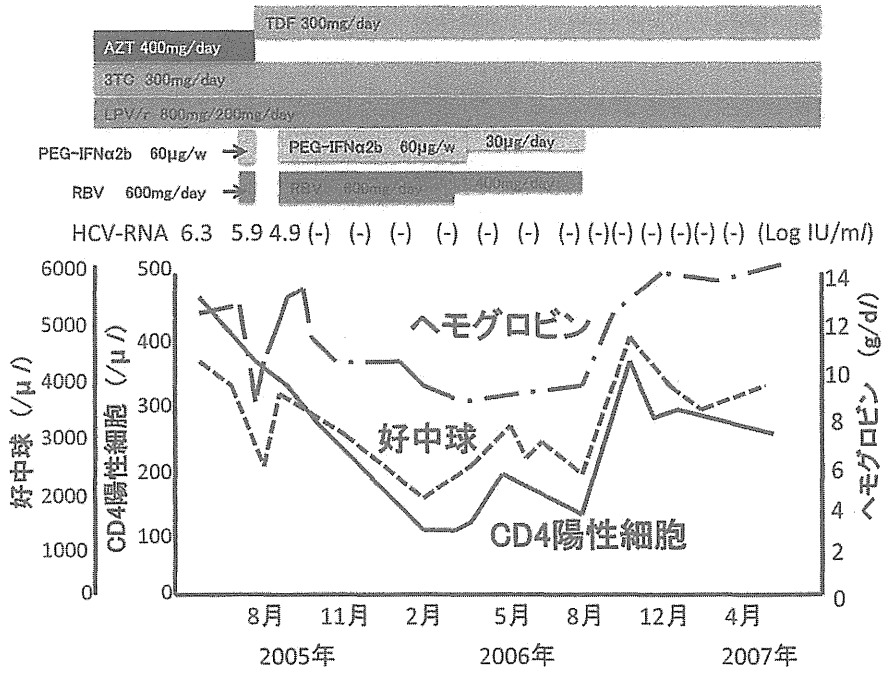

Figure 1. 症例6 治療経過：HIVに対するAZT，3TC，LPV/rによるHAART治療中にペグインターフェロン，リバビリン併用療法を開始したが，急激なヘモグロビン値，好中球数の減少を認め，著しい倦怠感を訴えた．ペグインターフェロン，リバビリン併用療法を中止とし，AZTをTDFに変更し，血球数の回復を待ってからペグインターフェロン，リバビリン併用療法を再開した．その後は，血球減少を認めるも48週間の治療を完遂できSVRが得られた．AZT；ジドブジン，TDF；テノホビル，3TC；ラミブジン，LPV/r；ロピナビル（少量リトナビル含有），PEG-IFNα2b；ペグインターフェロンα2b，RBV；リバビリン．

われた．なお，症例3はHAARTに対するadherenceが不良なため，治療中にHIVの再活性化が認められたが，CD4陽性細胞数は200/μl以上を維持していた．

今回の検討対象の母集団である当院におけるHIV，HCV重複感染例のうち27例でHCV genotypeを検討した．非加熱血液製剤による感染症例12症例では，genotype 1aが8例（66.7%）と最も多く，3aが2例（16.7%），1bおよび2aがそれぞれ1例（8.3%）であった．一方，非加熱血液製剤以外での感染症例15症例では，genotype 1bが6例（40.0%）と最も多く，1aおよび3bがそれぞれ2例（13.3%），2b，2c，3a，4a，6nがそれぞれ1例（6.7%）であった（Table 3）．

Ⅳ 考 察

今までのところ，HIV，HCV重複感染におけるC型慢性肝炎治療は，HCV単独感染と同様にPEG-IFN，RBV併用療法を中心に行われてきている．一般にHIV，HCV重複感染症例でのPEG-IFN，RBV併用療法は，HCV単独感染肝炎と比較して著効率が低いとされているが，その理由は十分には明らかにされていない．実際の治療に当たっては，治療導入時に十分なCD4陽性細胞数を有することが抗HCV治療の成績向上につながるとの報告もあり[7]，必要に応じてHAARTを併用することが推奨されている[8]．その際にHAARTとの薬物相互作用による有害事象に留意しつつ，十分な量の抗HCV薬を十分な期間投与することが重要と考えられている[9]．

今回，当院でのHIV，HCV重複感染症例におけるC型慢性肝炎に対するPEG-IFN，RBV併用療法の現状を検討したところ，忍容性にはおおむね問題がなかった．一部症例でHIVに対する治療内容の変更を必要としたが，重篤な合併症は経験しなかった．なお，一般にCD4陽性細胞数が200/μl以下の場合は，日和見感染の危険が高く

Table 3. 当院における HIV/HCV 重複感染者の HCV genotype

HCV genotype	感染経路 非加熱血液製剤 (n=12)	非加熱血液製剤以外 (n=15)	全体 (n=27)
1a	8 (66.7%)	2 (13.3%)	10 (37.0%)
1b	1 (8.3%)	6 (40.0%)	7 (25.9%)
2a	1 (8.3%)	0 (0%)	1 (3.7%)
2b	0 (0%)	1 (6.7%)	1 (3.7%)
2c	0 (0%)	1 (6.7%)	1 (3.7%)
3a	2 (16.7%)	1 (6.7%)	3 (11.1%)
3b	0 (0%)	2 (13.3%)	2 (7.4%)
4a	0 (0%)	1 (6.7%)	1 (3.7%)
6n	0 (0%)	1 (6.7%)	1 (3.7%)

なるといわれており，HCV に対する IFN を用いた治療の導入は推奨されず，HIV の治療が優先されている[10]．今回の症例は，治療開始時においては全例その基準を満たしていた．一方，経過中にはすべての症例で白血球減少を認め，それにともなって CD4 陽性細胞数も減少を認めた．ただし，PEG-IFN の投与量は通常の C 型慢性肝炎治療に準じて好中球数に応じて適宜増減を行い，結果的にほぼ CD4 陽性細胞数に合わせた IFN 投与量の増減が行われていた．3 例で CD4 陽性細胞数 200/μl を下回ったが，治療中の日和見感染の合併症は認めなかった．一般に，IFN 投与時に CD4 陽性細胞数の減少を認めても T リンパ球におけるその割合は低下せず，易感染症をきたすことはないとされており，IFN の減量基準も通常の基準に従えば問題がないと考えられた[11)12)]．

治療を受けた症例の HCV genotype は 1 が 3 例，4 が 1 例でそれら以外が 6 例であった．PEG-IFN，RBV 併用療法導入に当たって，genotype 1 および 4 の症例には難治が予測されることを説明してはいるが，なるべく積極的に導入する方向で対応している．しかし，当院における HIV, HCV 重複感染症例で HCV genotype の検討を行った 27 例のうち，genotype 1 または 4 の症例は，今回 HCV の治療を受けた症例では 10 例中 4 例 (40.0%) で，受けなかった症例では 17 例中 14 例 (82.4%) であった．今回治療を受けた症例のうち母集団の中では最も多い genotype 1 の症例が少なかったのは，難治が予測され治療開始を躊躇する症例が多かった結果と考えられる．広く知られるように世界的に HCV genotype は，1a および 1b が最も多く，次に 2a, 2b, 3a, 3b が多いといわれている[13]．わが国では genotype 1b が最も多く，2a, 2b が次に多い[14]．ただし，わが国における血友病症例などでの輸入非加熱血液製剤による感染では，1a, 1b がそれぞれ約 30%，3a が約 20% と推測されている[15]．当院で治療経過観察中の輸入非加熱血液製剤による感染症例では，12 例のうち genotype 1a が 8 例 (66.7%) と最も多かった．一方，血液製剤以外の感染症例 15 症例では genotype 1b が 6 例 (40.0%) と最も多く，それ以外では 1a, 3b がそれぞれ 2 例 (13.3%)，2b, 2c, 3a, 4a, 6n がそれぞれ 1 例 (6.7%) と多様であった．HIV, HCV 重複感染症例の中でも血液製剤以外での感染症例における genotype の多様性は，国外での感染や，国内においても経静脈麻薬常習者や，男性同性愛者などの外国人を含む狭いコミュニティでの感染であることに関連していると思われる．今回，治療を受けた患者のうち 5 症例は海外での感染と推測され，うち 3 症例 (症例 3, 7, 8) は海外出身者であった．推定感染地域から考えても，今回の症例群は日本での HCV 単独感染例における感染経路とは異なり，その結果 genotype の分布も異なる結果となっている．今回当院での HIV, HCV 重複感染で PEG-IFN, RBV 併用療法を施行した症

例のうちgenotype 1bは3例のみと少なく，その他の症例では多彩なgenotypeを認めたが，このことはHIV，HCV重複感染におけるgenotypeが多様であるという側面と，genotype 1の症例での治療導入率が低いという2点が関与していたと考えられる．

今回の治療効果としてはgenotype 1または4の症例ではSVRを認めたのは1例のみで，結果としては芳しいものではなかった．一方，genotype 1または4以外の症例では治療効果は良好で，多くの症例でSVRを認めた．この結果は，HCV単独感染症例で予測されるものと同様な結果であった[16)~18)]．

SVRが得られなかった症例を検討すると，症例1のgenotype 1b症例では，薬剤のadherenceも良好であったが，48週投与にてHCV-RNA量はほとんど低下を認めず，難治症例と考えられた．また，症例3のgenotype 1b症例では，治療開始当初はHCV-RNAの早期陰性化を認めたが，その後は治療中にもかかわらず，HCV-RNAの再活性化を認めbreakthrough hepatitisを呈し32週で治療中断となった．なお，本症例におけるHCV-RNAの再陽性化の理由は不明であった．症例8のgenotype 3b症例では，治療当初から好中球減少が著しく，PEG-IFNのadherenceが低く12週の時点でHCV-RNA量の変化をほとんど認めなかったため治療中断となった．症例9のgenotype 4a症例においては，16週でHCV-RNAの陰性化を認め，48週以上の投与を目標に治療を行っていたがインフルエンザ様症状による全身倦怠感が高度で，24週の時点で治療を中断した．そして，中断後に短期間で再燃している．一般にgenotype 4については，比較的難治であることが報告されており，genotype 1に準じた長期間の治療が必要とされている[19)]．

同療法の治療期間については，2011年に発表されたわが国の抗HIV治療ガイドラインにおいて，HCV-HIV International Panelによる2007年の勧告に準じたresponse guided therapyが推奨されている[10)20)]．具体的には，HCV-RNAが4週目に陰性のrapid virological response（RVR）を認めれば，genotype 1または4で48週間，1または4以外で24週間の投与が推奨されている．一方，4週目に陽性で12週目に2log以上の低下を認め24週までに陰性化した場合は，genotype 1または4で72週間，1または4以外で48週間の投与が推奨されている．なお，上記の条件に当てはまらない場合は，その時点での治療の中止が妥当とされている．今回の症例のうち副作用や治療反応性不良で中止した3症例（症例3，8，9）を除いた7症例中6症例でSVRを認めているが，それら6症例についてガイドラインで示された内容と比較検討すると，genotype 1または4でSVRを達成した1症例（症例2）では，RVRを認めた後，ガイドラインと合致した48週投与にてSVRを達成している．一方，genotype 1または4以外でSVRを達成した5症例では，1例（症例7）でRVRを経て24週投与，3例（症例4，6，10）で8週目のウイルス陰性化を経て48週投与と，ガイドラインに合致した治療でいずれもSVRを認めた．一方で，1例（症例5）では8週目のウイルス陰性化を経て，ガイドラインより短い24週投与にてSVRを認めている．ここで注目すべきなのは，genotype 1または4以外の2例（症例4，6）でPEG-IFN，RBVのadherenceは決して良好ではなかったが，単独感染の投与期間より長い48週間の投与を行ったところSVRを認めていることである．両症例ともHCV-RNAの陰性化時期は5週目以降で，結果的には現在のガイドラインに沿った形での治療を行っていた．ガイドラインに示されているresponse guided therapyでは，単独感染よりやや長めの投与期間が設定されているが，adherenceが比較的不良な症例に対しても対応可能な内容と考えられ，現在当院でも，この内容に沿った治療が行われている．

今回治療を受けたgenotype 1bの症例のうち，PEG-IFNα2a，RBV併用療法の保険適応が認められた2007年以降に治療を開始された症例が1例（症例2）のみあったが，全例PEG-IFNα2bを用いた治療が行われた．一般にPEG-IFN，RBV併用療法において，PEG-IFNα2aを用いる方がPEG-IFNα2bでの治療よりもわずかにSVR率が

高く有害事象は同程度との報告が多い[21)22)]．一方，HIV，HCV重複感染症例では，両薬剤のSVR率に差がなく，PEG-IFNα2aの方がより血球減少が高度であるとの報告もある[23)]．前出のガイドラインにおいても，PEG-IFN，RBV併用療法においてPEG-IFNαの種類にまでは言及しておらず，症例ごとに各薬剤の特徴を考慮して使用すべきと考えられる[10)]．

また，本療法の注意事項として，PEG-IFNおよびRBVと抗HIV剤との相互作用についての報告も散見されている．一般に抗HIV剤はPEG-IFNとの相互作用はないとされているが，一方でいくつかの抗HIV剤はRBVとの相互作用が報告されており注意が必要である[24)]．特に核酸系逆転写酵素阻害剤であるAZTは血液毒性が比較的高度であるが，RBVとの併用で重篤な貧血をおこすことから原則併用禁忌である[3)25)]．今回，AZTを使用した状態でPEG-IFN，RBV併用療法が開始されたことにより，急速に貧血を呈し一時PEG-IFN，RBV併用療法が中止となった症例（症例6）が存在した．その後，AZTをTDFに変更することで速やかに貧血は改善しPEG-IFN，RBVの48週間投与を行うことができた[26)]．当院ではHIVの治療を感染症科が，HCVの治療を消化器科が担当している．消化器科医師はHAARTに慣れておらず，AZTとRBV併用の危険性に対する認識がなかった．今後，HIVとHCVに対する治療者が異なる場合は，消化器科の医師もHAARTに対する十分な理解が必要で，HIVに対する治療者との綿密な情報交換が必須と思われた．また，核酸系逆転写酵素阻害剤であるジダノシン（ddi）とサニルブジン（d4T）は，ミトコンドリア障害による乳酸アシドーシスや膵炎を生ずる危険があり，RBVとの併用で細胞内濃度が上昇することでその頻度が増大すると報告されており，特にddiは併用禁忌である[27)]．今回，1例（症例10）において，患者の希望で前医からの処方を変更できずにd4Tを使用したままPEG-IFN，RBV併用療法を行った．幸い重篤な合併症は生じなかったが，PEG-IFN，RBV併用療法開始前にddiやd4Tを使用している症例は他の薬剤に変更してから治療を開始するべきと思われる．ただし，他の核酸系逆転写酵素阻害剤においても乳酸アシドーシスや膵炎のリスクは存在しており，血中乳酸値を測定するなどの注意を払って治療に当たるべきである．一方，核酸系逆転写酵素阻害剤であるアバカビル（ABC）はRBVと代謝経路が一部同じであるため，競合的リン酸化阻害によるRBVの効果減弱の可能性が指摘されているが，実際の治療効果への影響は不明である[28)]．また，プロテアーゼ阻害剤であるアタナザビル（ATV）を使用中にPEG-IFN，RBV併用療法を行うと，高度のビリルビン血症をきたすことがあるとの報告もあり注意が必要である[29)]．

相互作用ではないが，非核酸系逆転写酵素阻害剤であるEFVは抑鬱などの精神神経症状をきたしやすいため，PEG-IFN投与に当たっては他剤への変更が望ましいとされている[30)]．今回の症例でも3症例でEFVが使用されていたが，PEG-IFN，RBV併用療法の開始に当たって2症例で薬剤の変更が行われていた．

今後の展望としては，HCVに対するプロテアーゼ阻害剤であるテラプレビルとの併用によるC型慢性肝炎の治癒率向上が期待されている[31)]．HIV，HCV genotype 1重複感染例に対するテラプレビル，PEG-IFN，RBV併用療法のphase II trialの途中経過の報告では，重篤な有害事象はなく，4週，12週の時点でHCV-RNA陰性化率はいずれも約70%と報告されており，最終の結果が期待されている[32)]．ただし，抗HIV剤とテラプレビルとの薬剤相互作用も報告されており注意が必要である．テラプレビルは，リトナビルをブースターとした各種抗HIVプロテアーゼ阻害剤やEFVの使用で血中濃度が低下するとの報告がある[33)]．また，テラプレビルはTDFの血中濃度の上昇をもたらすため定期的な腎機能の観察が必要とも報告されている[33)34)]．しかし，今のところHIV，HCV重複感染症例に対するテラプレビルの投与についての報告は限られており，抗HIV剤との相互作用の全貌が明らかになっているとはいい難く，現在も検討途中の段階である[35)]．

結　論

HIV と HCV の重複感染症例の治療は，HIV 感染症治療の中でも重要な位置づけを有しており，消化器科医の果たす役割は大きい．今回の検討で HIV，HCV の重複感染症例に対する PEG-IFN，RBV 併用療法は，適切な抗 HIV 療法のもとで行えば安全で有効な治療と考えられた．特に，genotype 1 または 4 以外の症例では，単独感染より長期間の治療を行うことで良好な治療成績を得ることができた．今後は，genotype 1 高ウイルス症例を主とした難治例に対するテラプレビル，PEG-IFN，RBV 併用療法による治療成績の向上が期待されている．

謝辞：本研究に際し，ご指導，ご尽力いただきました愛知県赤十字血液センター濱口元洋先生にこの場を借りて深謝申し上げます．

なお，本論文の要旨は，第 96 回日本消化器病学会総会（2010 年 4 月 23 日，新潟市）にて報告した．

本論文内容に関連する著者の利益相反
：後藤秀実（MSD 株式会社）

文　献

1) Koike K, Tsukada K, Yotsuyanagi H, et al : Prevalence of coinfection with human immunodeficiency virus and hepatitis C virus in Japan. Hepatol Res 37 ; 2–5 : 2007
2) Tatsunami S, Mimaya J, Shirahata A, et al : Current status of Japanese HIV-infected patients with coagulation disorders : coinfection with both HIV and HCV. Int J Hematol 88 ; 304–310 : 2008
3) Fuster D, Huertas JA, Gómez G, et al : Baseline factors associated with haematological toxicity that leads to a dosage reduction of pegylated interferon-alpha2a and ribavirin in HIV- and HCV-coinfected patients on HCV antiviral therapy. Antivir Ther 10 ; 841–847 : 2005
4) Núñez M, Ocampo A, Aguirrebengoa K, et al : Incidence of anaemia and impact on sustained virological response in HIV/HCV-coinfected patients treated with pegylated interferon plus ribavirin. J Viral Hepat 15 ; 363–369 : 2008
5) Felsenstein J : Evolutionary trees from DNA sequences : a maximum likelihood approach. J Mol Evol 17 ; 368–376 : 1981
6) Li C, Fu Y, Lu L, et al : Complete genomic sequences for hepatitis C virus subtypes 6e and 6g isolated from Chinese patients with injection drug use and HIV-1 co-infection. J Med Virol 78 ; 1061–1069 : 2006
7) Avidan NU, Goldstein D, Rozenberg L, et al : Hepatitis C viral kinetics during treatment with peg IFN-alpha-2b in HIV/HCV coinfected patients as a function of baseline CD4+ T-cell counts. J Acquir Immune Defic Syndr 52 ; 452–458 : 2009
8) European Association for the Study of the Liver : EASL Clinical Practice Guidelines : management of hepatitis C virus infection. J Hepatol 55 ; 245–264 : 2011
9) Cargnel A, Angeli E, Mainini A, et al : Open, randomized, multicentre italian trial on PEG-IFN plus ribavirin versus PEG-IFN monotherapy for chronic hepatitis C in HIV-coinfected patients on HAART. Antivir Ther 10 ; 309–317 : 2005
10) 平成 22 年度厚生労働科学研究費補助金エイズ対策研究事業，HIV 感染症及びその合併症の課題を克服する研究班：抗 HIV 治療ガイドライン，104–105 : 2011
11) Torriani FJ, Rodriguez-Torres M, Rockstroh JK, et al : Peginterferon Alfa-2a plus ribavirin for chronic hepatitis C virus infection in HIV-infected patients. N Engl J Med 351 ; 438–450 : 2004
12) Taylor JM, Fahey JL, Detels R, et al : CD4 percentage, CD4 number and CD4 : CD8 ratio in HIV infection : which to choose and how to use. J Acquir Immune Defic Syndr 2 ; 114–124 : 1989
13) Zein NN : Clinical significance of hepatitis C virus genotypes. Clin Microbiol Rev 13 ; 223–235 : 2000
14) Yamada G, Tanaka E, Miura T, et al : Epidemiology of genotypes of hepatitis C virus in Japnanese patients with type C chronic liver diseases : a multi-institution analysis. J Gastroenterol Hepatol 10 ; 538–545 : 1995
15) 小池和彦，高松純樹，菅原寧彦，他：我が国における HIV 感染症に合併する HCV 感染症の実態．厚生労働省科学研究費助成金　エイズ対策研究事業　平成 15 年度～17 年度　総合研究報告書，23–34 : 2005
16) Fried MW, Shiffman ML, Reddy KR, et al : Peginterferon alfa-2a plus ribavirin for chronic hepatitis C virus infection. N Engl J Med 347 ; 975–982 : 2002
17) Zeuzum S : Heterogeneous virologic response rates to interferon-based therapy in patients with chronic hepatitis C : who responds less well? Ann Intern Med 140 ; 370–381 : 2004
18) Zhao S, Cheng D, Liu E, et al : Peginterferon vs.

interferon in the treatment of different HCV genotype infections in HIV patients. Eur J Clin Microbiol Infect Dis 27 ; 1183–1192 : 2008
19) Martín-Carbonero L, Puoti M, García-Samaniego J, et al : Response to pegylated interferon plus ribavirin in HIV-infected patients with chronic hepatitis C due to genotype 4. J Viral Hepat 15 ; 710–715 : 2008
20) Soriano V, Puoti M, Sulkowski M, et al : Care of patients coinfected with HIV and hepatitis C virus : 2007 updated recommendations from the HCV-HIV International Panel. AIDS 21 ; 1073–1089 : 2007
21) Rumi MG, Aghemo A, Prati GM, et al : Randomized study of peginterferon-alpha2a plus ribavirin vs peginterferon-alpha2b plus ribavirin in chronic hepatitis C. Gastroenterology 138 ; 108–115 : 2010
22) Awad T, Thorlund K, Hauser G, et al : Peginterferon alpha-2a is associated with higher sustained virological response than peginterferon alfa-2b in chronic hepatitis C : systematic review of randomized trials. Hepatology 51 ; 1176–1184 : 2010
23) Laguno M, Cifuentes C, Murillas J, et al : Randomized trial comparing pegylated interferon alpha-2b versus pegylated interferon alpha-2a, both plus ribavirin, to treat chronic hepatitis C in human immunodeficiency virus patients. Hepatology 49 ; 22–31 : 2009
24) Seden K, Back D, Khoo S : New directly acting antivirals for hepatitis C : potential for interaction with antiretrovirals. J Antimicrob Chemother 65 ; 1079–1085 : 2010
25) Mira JA, López-Cortés LF, Merino D, et al : Predictors of severe haematological toxicity secondary to pegylated interferon plus ribavirin treatment in HIV-HCV-coinfected patients. Antivir Ther 12 ; 1225–1235 : 2007
26) 高橋昌明, 藤崎誠一郎, 伊部史朗, 他 : HIV, HCV 重複感染に対するリバビリン併用ペグインターフェロン療法により CD4, CD8 陽性リンパ球数が減少した1症例. 新薬と臨床 56 ; 332–335 : 2007
27) Bani-Sadr F, Carrat F, Pol S, et al : Risk factors for symptomatic mitochondrial toxicity in HIV/hepatitis C virus-coinfected patients during interferon plus ribavirin-based therapy. J Acquir Immune Defic Syndr 40 ; 47–52 : 2005
28) Mira JA, López-Cortés LF, Barreiro P, et al : Efficacy of pegylated interferon plus ribavirin treatment in HIV/hepatitis C virus co-infected patients receiving abacavir plus lamivudine or tenofovir plus either lamivudine or emtricitabine as nucleoside analogue backbone. J Antimicrob Chemother 62 ; 1365–1373 : 2008
29) Rodríguez-Nóvoa S, Morello J, González M, et al : Increase in serum bilirubin in HIV/hepatitis-C virus-coinfected patients on atazanavir therapy following initiation of pegylated-interferon and ribavirin. AIDS 22 ; 2535–2537 : 2008
30) Laguno M, Blanch J, Murillas J, et al : Depressive symptoms after initiation of interferon therapy in human immunodeficiency virus-infected patients with chronic hepatitis C. Antivir Ther 9 ; 905–909 : 2004
31) Soriano V, Sherman KE, Rockstroh J, et al : Challenges and opportunities for hepatitis C drug development in HIV-hepatitis C virus-co-infected patients. AIDS 25 ; 2197–2208 : 2011
32) Sulkowski M, Dietrich D, Sherman K, et al : Interim analysis of a phase 2a double-blind study of TVR in combination with pegIFN-α2a and RBV in HIV/HCV co-infected patients. 18th CROI, 146LB : 2011
33) Van Heeswijk R, Vandevoorde A, Boogaerts G, et al : Pharmacokinetic Interactions between ARV Agents and the Investigational HCV Protease Inhibitor TVR in Healthy Volunteers. 18th CROI, 119 : 2011
34) Van Heeswijk R, Gysen V, Boogaerts G, et al : The pharmacokinetic interaction between tenofovir disoproxil fumarate and the investigational HCV protease inhibitor telaprevir. 48th ICAAC, 13–17 : 2008
35) Thomas DL, Bartlett JG, Peters MG, et al : Provisional guidance on the use of hepatitis C virus protease inhibitors for treatment of hepatitis C in HIV-infected persons. Clin Infect Dis 54 ; 979–983 : 2011

（論文受領, 2011年9月5日
受理, 2012年1月29日）

Clinical evaluation of peginterferon α plus ribavirin for patients co-infected with HIV and HCV at Nagoya Medical Center

Tomoyuki TSUZUKI, Hiroaki IWASE, Masaaki SHIMADA[1], Noboru HIRASHIMA[2], Yusuke HIBINO, Nobumitsu RYUGE, Masashi SAITO, Dai TAMAKI, Asako KAMIYA, Misaki YOKOI[1], Yoshiyuki YOKOMAKU[3], Seiichiro FUJISAKI[4], Wataru SUGIURA[5] and Hidemi GOTO[6]

[1] *Department of Gastroenterology, National Hospital Organization, Nagoya Medical Center*
[2] *Department of Gastroenterology, National Hospital Organization, East Nagoya Hospital*
[3] *Department of Infectious Diseases, National Hospital Organization, Nagoya Medical Center*
[4] *Influenza Virus Research Center, National Institute of Infectious Disease*
[5] *Clinical Research Center, National Hospital Organization, Nagoya Medical Center*
[6] *Department of Gastroenterology, Nagoya University Graduate School of Medicine*

At Nagoya Medical Center, 10 patients co-infected with HIV and HCV received peginterferon α (PEG-IFNα) plus ribavirin therapy. Three of the cases were HCV genotype 1b, 2 cases were HCV 3b, and 1 case each were 2b, 2c, 3a, 4a and 6n. Nine patients received anti HIV therapy from the beginning. In 5 of these patients, anti HIV therapy was modified when PEG-IFNα plus ribavirin treatment was started. Of the above, 7 patients completed the protocol. No patients had severe adverse effects. Sustained virological response was achieved in 1 of 4 (25%) of the patients with genotypes 1 or 4, and in 5 of 6 (83%) of the patients with other genotypes. PEG-IFNα plus ribavirin therapy is considered a safe and efficacious treatment for patients co-infected with HIV and HCV.

Published online 8 September 2011

Nucleic Acids Research, 2012, Vol. 40, No. 1 **345–359**
doi:10.1093/nar/gkr694

Biochemical, inhibition and inhibitor resistance studies of xenotropic murine leukemia virus-related virus reverse transcriptase

Tanyaradzwa P. Ndongwe[1], Adeyemi O. Adedeji[1], Eleftherios Michailidis[1], Yee Tsuey Ong[1], Atsuko Hachiya[1], Bruno Marchand[1], Emily M. Ryan[1], Devendra K. Rai[1], Karen A. Kirby[1], Angela S. Whatley[1], Donald H. Burke[1,2], Marc Johnson[1], Shilei Ding[3], Yi-Min Zheng[1], Shan-Lu Liu[1,3], Ei-Ichi Kodama[4], Krista A. Delviks-Frankenberry[5], Vinay K. Pathak[5], Hiroaki Mitsuya[6], Michael A. Parniak[7], Kamalendra Singh[1] and Stefan G. Sarafianos[1,2,*]

[1]Christopher Bond Life Sciences Center, Department of Molecular Microbiology & Immunology, University of Missouri, School of Medicine, Columbia, [2]Department of Biochemistry, University of Missouri, Columbia, MO 65211, USA, [3]Department of Microbiology and Immunology, McGill University, Montreal, QC, Canada, [4]Department of Internal Medicine, Division of Emerging Infectious Diseases, Tohoku University School of Medicine, Sendai, Japan, [5]HIV Drug Resistance Program, National Cancer Institute-Frederick, Frederick MD, [6]Department of Internal Medicine, Kumamoto University School of Medicine, Kumamoto Japan & Experimental Retrovirology Section, HIV/AIDS Malignancy Branch, NIH, Bethesda MD and [7]Department of Molecular Genetics & Biochemistry, University of Pittsburgh School of Medicine, Pittsburgh, PA, USA

Received June 3, 2011; Revised August 5, 2011; Accepted August 8, 2011

ABSTRACT

We report key mechanistic differences between the reverse transcriptases (RT) of human immunodeficiency virus type-1 (HIV-1) and of xenotropic murine leukemia virus-related virus (XMRV), a gammaretrovirus that can infect human cells. Steady and pre-steady state kinetics demonstrated that XMRV RT is significantly less efficient in DNA synthesis and in unblocking chain-terminated primers. Surface plasmon resonance experiments showed that the gammaretroviral enzyme has a remarkably higher dissociation rate (k_{off}) from DNA, which also results in lower processivity than HIV-1 RT. Transient kinetics of mismatch incorporation revealed that XMRV RT has higher fidelity than HIV-1 RT. We identified RNA aptamers that potently inhibit XMRV, but not HIV-1 RT. XMRV RT is highly susceptible to some nucleoside RT inhibitors, including Translocation Deficient RT inhibitors, but not to non-nucleoside RT inhibitors. We demonstrated that XMRV RT mutants K103R and Q190M, which are equivalent to HIV-1 mutants that are resistant to tenofovir (K65R) and AZT (Q151M), are also resistant to the respective drugs, suggesting that XMRV can acquire resistance to these compounds through the decreased incorporation mechanism reported in HIV-1.

INTRODUCTION

Xenotropic murine leukemia virus-related virus (XMRV) is a gammaretrovirus that was first identified in some prostate cancer tissues (1,2) While some subsequent reports confirmed the presence of XMRV in prostate cancer samples (3–6), several others found little or no evidence of the virus in patient samples (7–9). XMRV DNA was also reported in 67% of patients with chronic fatigue syndrome (CFS) (10), but several subsequent studies in Europe and the USA failed to identify XMRV DNA in CFS patients or healthy controls (11–15). Hence, the relevance of XMRV to human disease remains unclear (16) and have been challenged (17). Most recently, it has been reported that XMRV has been generated through recombination of two separate proviruses suggesting that the association of XMRV with human disease is due to contamination of human samples with virus originating from this recombination event (18). Nonetheless, as a retrovirus that can infect human cells, XMRV can be very helpful in advancing our understanding of the mechanisms of retroviral reverse transcription, inhibition and drug resistance.

*To whom correspondence should be addressed. Tel: +1 573 882 4338; Fax: +1 573 884 9676; Email: sarafianoss@missouri.edu

XMRV RT is similar to the Moloney murine leukemia virus (MoMLV) RT, which has been the subject of structural and biochemical studies (19–24). Most of the differences between these gammaretroviral enzymes are at the RNase H domain (Supplementary Figure S1). Comparisons of human immunodeficiency virus type-1 (HIV) RT with MoMLV RT have revealed structural and sequence differences (21). For example, HIV-1 RT is a heterodimer composed of two related subunits (25,26) [reviewed in (27,28)]. Its larger p66 subunit (~66 kDa) contains both the polymerase and RNase H domains; the smaller p51 subunit, (~51 kDa), is derived from the p66 subunit by proteolytic cleavage and its role is to provide structural support and optimize RT's biochemical functions (29). In contrast, structural studies have demonstrated that MoMLV RT is a monomer of about 74 kDa, although one study reported that it may form a homodimer during DNA synthesis (30). So far, there are no published biochemical or structural studies on XMRV RT. Hence, the present study on this enzyme and its comparison to related enzymes provides an excellent opportunity to advance our biochemical understanding of the mechanism of reverse transcription, its inhibition and drug resistance.

MATERIALS AND METHODS

Expression and purification of XMRV, HIV-1 and MoMLV RTs

The plasmid pBSK-XMRV containing the coding sequence of XMRV RT from the VP62 clone (GenBank: DQ399707.1) was chemically synthesized and optimized for bacterial expression by Epoch Biolabs Inc (Missouri City, Texas, USA). The 2013 bp XMRV RT sequence was amplified from pBSK-XMRVRT by PCR, using the forward and reverse primers 1 (all primer sequences are shown in Supplementary Table S1), resulting in NdeI and HindIII restriction sites. Drug resistant XMRV RT mutants Q190M and K103R (equivalent to HIV-1 Q151M RT and K65R) were generated by site-directed mutagenesis using forward and reverse primers 2 and 3. The digested amplicons were ligated into pET-28a (Novagen), resulting into a construct that expresses an N-terminal hexahistidine tag. pET-28a-MRT encoding full-length wild-type MoMLV RT was provided by Dr M. Modak (New Jersey Medical School, Newark NJ, USA).

Expression and purification of MoMLV and XMRV RTs were carried out similarly to our previously published protocols (23,24). Briefly, RTs were expressed in BL21-pLysS *Escherichia coli* (Invitrogen) grown at 37°C and induced with 150 μM IPTG at OD_{600} 0.8, followed by 16 h growth at 17°C. A cell pellet from a 3 l culture was incubated with 40 ml lysis buffer (50 mM Tris–HCl, pH 7.8, 500 mM NaCl, 1 mM PMSF, 0.1% NP-40, 1% sucrose and 2 mg/ml lysozyme), then sonicated and centrifuged at 15,000 *g* for 30 min. The supernatant was diluted 2-fold in Buffer A (50 mM Tri–HCl pH 7.8, 1 mM PMSF, 4% streptomycin sulfate and 10% sucrose), stirred on ice for 30 min and centrifuged. The supernatant was loaded on a Ni-NTA column and bound proteins were washed with 20 ml Buffer B (20 mM Tris–HCl pH 7.5, 500 mM NaCl) and 5 mM imidazole, followed by 20 ml Buffer B with 75 mM imidazole. RT was eluted in 2 ml fractions with 20 ml buffer B containing 300 mM imidazole. Fractions with RT were pooled and further purified by size exclusion chromatography (Superdex 75; GE Healthcare). RTs (>95% pure) were stored in 50 mM Tris–HCl pH 7.0, 100 mM NaCl, 1 mM DTT, 0.1% NP-40 and 30% glycerol in 10 μl aliquots at −20°C. Protein concentrations were determined by measuring UV_{280} (molar extinction coefficients of 106 and 103 $M^{-1}cm^{-1}$ for XMRV and MoMLV RT).

HIV-1 RT was cloned in a pETduo vector and purified as described previously (29,31,32). Oligonucleotide sequences (IDT-Coralville, IA, USA) of DNA/RNA substrates are shown in Supplementary Table S1. Nucleotides were purchased from Fermentas (Glen Burnie, MD, USA). They were treated with inorganic pyrophosphatase (Roche Diagnostics, Mannheim, Germany) as described previously (33) to remove PPi that might interfere with excision assays.

Steady state kinetics

Steady state parameters K_m and k_{cat} for dATP incorporation were determined using single nucleotide incorporation gel-based assays. XMRV RT and MoMLV RT reactions were carried out in 50 mM Tris–HCl pH 7.8, 60 mM KCl, 0.1 mM DTT, 0.01% NP-40 and 0.01% bovine serum albumin (BSA) (Reaction Buffer) with 6 mM $MgCl_2$ or 1.5 mM $MnCl_2$, 0.5 mM EDTA, 200 nM or 100 nM T_{d26}/5′-Cy3-P_{d18b}, 20 nM or 5 nM RT for XMRV and MoMLV RTs, respectively and varying concentrations of dNTP in a final volume of 10 μl. The reactions for HIV-1 RT were carried out in Reaction Buffer with 100 nM T_{d26}/5′-Cy3-P_{d18b}, 10 nM HIV-1 RT and 6 mM $MgCl_2$ in a 20 μl reaction. All the concentrations mentioned here and in subsequent assays reflect final concentration of reactants otherwise mentioned reactions were stopped after 15 min for XMRV, 4 min for MoMLV RT, and 2.5 min for HIV-1. The products were resolved on 15% polyacrylamide–7M urea gels. The gels were scanned with a Fuji Fla-5000 PhosphorImager (Stamford, CT, USA) and the bands were quantified using MultiGauge. Results were plotted using GraphPad Prism 4. K_m and k_{cat} were determined graphically using Michaelis–Menten equation.

Gel mobility shift assays

Formation of RT-DNA binary complex: 20 nM T_{d31}/5′-Cy3-P_{d18a} (Supplementary Table S1) was incubated for 10 minutes with increasing amounts of MoMLV or XMRV RT in 50 mM Tris–HCl pH 7.8, 0.01% BSA, 5 mM $MgCl_2$ and 10% (v/v) sucrose. The complexes were resolved on native 6% polyacrylamide 50 mM Tris–borate gel and visualized as described above.

Active site titration and determination of $K_{D.DNA}$

Active site concentrations and kinetic constants of DNA binding for XMRV, HIV-1 and MoMLV RTs were determined using pre-steady state experiments. Reactions

with XMRV and MoMLV RTs were carried out in the reaction buffers listed above. For XMRV RT 100 nM protein was pre-incubated with increasing concentrations of T_{d31}/5′-Cy3-P_{d18a}, followed by rapid mixing with a reaction mixture containing 5 mM $MgCl_2$ and 100 μM next incoming nucleotide (dATP). The reactions were quenched at various times (5 ms to 4 s) by adding EDTA to a final concentration of 50 mM. The amounts of 19-mer product were quantified and plotted against time. The data were fit to the following burst equation:

$$P = A(1 - e^{-k_{obs}t}) + k_{ss}t \quad (1)$$

where A is the amplitude of the burst phase that represents the RT–DNA complex at the start of the reaction, k_{obs} is the observed burst rate constant for dNTP incorporation, k_{ss} is the steady state rate constant and t is the reaction time. The rate constant of the linear phase (k_{cat}) was estimated by dividing the slope of the linear phase by the enzyme concentration. The active site concentration and T/P binding affinity ($K_{D.DNA}$) were determined by plotting the amplitude (A) against the concentration of T/P. Data were fit to the quadratic equation (Equation 2) using non-linear regression:

$$A = 0.5(K_D + [RT] + [DNA] - \sqrt{0.25(K_D + [RT] + [DNA])^2} - ([RT] + [DNA]) \quad (2)$$

where K_D is the dissociation constant for the RT–DNA complex, and [RT] is the concentration of active polymerase. HIV-1 RT's DNA binding affinity was determined as previously described (29).

Surface plasmon resonance assay

We used surface plasmon resonance (SPR) to measure the binding constants of XMRV and HIV-1 RTs to double-stranded DNA. Experiments were carried out using a Biacore T100 (GE Healthcare). To prepare the sensor chip surface we used the 5′-biotin-T_{d37}/P_{d25} oligonucleotide (Supplementary Table S1). One hundred and twenty RUs of this DNA duplex were bound in channel 2 of a streptavidin-coated sensor chip [Series S Sensor Chip SA (certified)] by flowing a solution of 0.1 μM DNA at a flow rate of 10 μl/min in a buffer containing 50 mM Tris pH 7.8, 50 mM NaCl. The binding constants were determined as follows: RT binding was observed by flowing solutions containing increasing concentrations of the enzyme (0.2, 0.5, 1, 2, 5, 10, 20, 50, 100 and 200 nM) in 50 mM Tris pH 7.8, 60 mM KCl, 1 mM DTT, 0.01% NP40 and 10 mM $MgCl_2$ in channels 1 (background) and 2 (test sample) at 30 μl/min. The trace obtained in channel 1 was subtracted from the trace in channel 2 to obtain the binding signal of RT. This signal was analyzed using the Biacore T100 Evaluation software to determine $K_{D.DNA}$, k_{on} and k_{off}.

Pre-steady state kinetics of dNTP incorporation

The optimal nucleotide incorporation rates (k_{pol}) were obtained by pre-steady state kinetics analysis using single nucleotide incorporation assays. A solution containing XMRV RT (150 nM final concentration) and T_{d31}/5′-Cy3-P_{d18a} (40 nM) was rapidly mixed with a solution of $MgCl_2$ (5 mM) and varying dATP (5–200 μM) for 0.1 to 6 s before quenching with EDTA (50 mM) (all concentrations in parentheses are final, unless otherwise stated). Products were resolved and quantified as described above. Burst phase incorporation rates and substrate affinities were obtained from fitting the data to Equation 1. Turnover rates (k_{pol}), dNTP binding to the RT-DNA complex ($K_{d.dATP}$), and observed burst rates (k_{obs}) were fit to the hyperbolic equation:

$$k_{obs} = (k_{pol}[dNTP])/(K_{d.dNTP} + [dNTP]) \quad (3)$$

HIV-1 RT's DNA binding affinity was determined as previously described (29).

Fidelity of DNA synthesis

The fidelity (error-proneness) of XMRV RT was determined and compared with that of MoMLV RT and HIV-1 RT by primer extension assays using 10 nM heteropolymeric T_{d100}/5′-Cy3-P_{d18a}. Reactions (10 μl) were carried out in Reaction Buffer containing all four dNTPs (100 μM each) or only three dNTPs (missing either dATP, dGTP or dTTP) at 100 μM each. Incubations of the XMRV and MoMLV (50 nM) reactions were at 37°C for 45 min and 30 min for HIV-1 RT (20 nM). Reactions were initiated by adding dNTPs, stopped with equal volume of formamide-bromophenol blue, and an aliquot was run on a 16% polyacrylamide–7M urea gel.

Kinetics of mismatch incorporation

For these experiments, instead of including the next correct nucleotide (dATP) in the polymerase reactions, we used dTTP as the mismatched incoming nucleotide. Hence, 50 nM XMRV RT was pre-incubated with 35 nM T_{d31}/5′-Cy3-P_{d18a} in reaction mixture. Reactions were initiated by adding dTTP (5–750 μM) and 5 mM $MgCl_2$, followed by incubation (37°C) for 5 min, due to the decreased mismatch incorporation rate of XMRV. For MoMLV RT, 30 nM RT and 20 nM DNA used and the reactions were carried out for 2.5 minutes. For HIV-1, 30 nM RT, 20 nM DNA and 0–200 μM nucleotide were used and the reactions were carried out for 2.5 min. The amount of extended primer was quantified and plotted against the concentration of dTTP. The data were used to derive the $K_{d.dNTP}$ of incorrect nucleotide binding, the rate k_{pol} (using Equations 1 and 3) and the efficiency of the misincorporation reaction ($k_{pol}/K_{d.dTTP}$).

Determination of *in vivo* fidelity

ANGIE P cells, which contain a retroviral vector (GA-1) that encodes a bacterial β-galactosidase gene (*lacZ*) and a neomycin phosphotransferase gene, were plated (5×10^6 cells/100 mm dish) and after 24 h were transfected using the calcium phosphate precipitation method with a plasmid expressing either XMRV or amphotropic MLV (AM-MLV) (three independent transfections per vector). After 48 h, the culture medium with XMRV or (AM-MLV) was harvested, serially diluted and used to infect

D17 target cells (2×10^5 cells/60 mm dish) in the presence of polybrene. The infected D17 cells were selected for resistance to G418 (400 μg/ml) in the presence of 1 μM AZT to suppress reinfection, and characterized by staining with 5-bromo-4-chloro-3-indoyl-β-D-galacto-pyranoside (X-Gal) ~2 weeks after G418 selection. The frequencies of inactivating mutations in *lacZ* quantified as described before (blue versus white colonies) (34).

Processivity of DNA synthesis—trap assay

Processivity reactions were carried out in Reaction Buffer containing 20 nM T_{d100}/P_{d18}, 100 μM of each dNTP, 30 nM HIV-1 RT, 50 nM MoMLV RT or 100 nM XMRV RT and 1 μg/μl unlabeled calf thymus DNA trap in 50 μL. Enzymes were pre-incubated with T_{d100}/P_{d18} for 1 min before adding dNTPs (100 μM each) together with the calf thymus DNA trap. Reactions were incubated at 37°C, and 10 μl aliquots were taken out at 3, 7.5 and 15 min for HIV-1 RT or at 7.5, 15 and 30 min for XMRV RT and MoMLV RT, and mixed with equal volume of loading dye. The effectiveness of the trap was determined by pre-incubating the enzyme with the trap before adding T_{d100}/P_{d18}. Control DNA synthesis was measured in absence of trap under the same conditions. Reaction products were resolved as above.

Single turnover processivity assays

Thirty nanomolar $T_{d31}/5'$-Cy3-P_{d18a} was pre-incubated for 10 min with 100 nM XMRV or 50 nM MoMLV RT in Reaction Buffer, then rapidly mixed with 100 μM dNTPs, 5 mM $MgCl_2$ for varying times (0.1–45 s) before quenching with EDTA (50 mM final). Single turnover processivity of HIV-1 RT was assayed with 40 nM enzyme, 20 nM DNA and 50 μM of each nucleotide were used. The reaction products were resolved and quantified as described above. The data were fit to a one-phase exponential decay equation for the elongation of the 18-mer primer. The rates of appearance and extension of products from subsequent nucleotide incorporations (19- and 27-mer) were obtained by fitting the intensities of corresponding bands to double exponential (Equation 4):

$$P = A(1 - e^{-k_1 t}) + (e^{-k_2 t}) + C \quad (4)$$

where A is the amplitude, P is the amount of 19-mer, 20-mer or higher length products, k_1 is the rate of product generation, k_2 the rate of subsequent elongation and C a constant (29,35).

Assays for reverse transcriptase inhibition

DNA synthesis by 50 nM XMRV RT or MoMLV RT was carried out in Reaction Buffer using 20 nM $T_{d100}/5'$-Cy3-P_{d18a}, 2.5 μM dNTP, 5 mM $MgCl_2$ and varying amounts of NRTI (0–100 μM). Reactions were quenched with 95% formamide after 1 h incubation at 37°C (38). In experiments with aptamers 10 nM XMRV RT, 20 nM $T_{d31}/5'$-Cy3-P_{d18a} and 50 μM dNTPs were used in the presence of varying amounts of aptamer for 30 min (0–500 nM for m.1.3; 0–25 nM for m.1.4 and m.1.1FL). The inhibition of DNA polymerization was monitored by resolving the products on 15% polyacrylamide–7 M urea gels and visualized as described above. Bands corresponding to full extension products were quantified using MultiGauge Software and IC_{50}s were obtained from dose–response curves using GraphPad Prism.

PPi- and ATP-dependent excision and rescue of $T/P_{AZT\text{-}MP}$ or $T/P_{EFdA\text{-}MP}$

The ability of enzymes to use PPi or ATP to unblock template-primers that had AZT-MP ($T/P_{AZT\text{-}MP}$) or EFdA-MP ($T/P_{EFdA\text{-}MP}$) at their 3′ primer ends was measured as follows: 20 nM of $T/P_{AZT\text{-}MP}$ or $T/P_{EFdA\text{-}MP}$ were prepared as described before (32). They were incubated at 37°C with either 60 nM HIV-1 RT or 200 nM XMRV RT in the presence of 0.15 mM PPi or 3.5 mM ATP for PPi- or ATP-dependent rescue reactions, respectively. Reactions were initiated by the addition of $MgCl_2$ (6 mM). Aliquots were removed at different times (0–90 min) and analyzed as above. Rescue assays were performed in the presence of 100 μM dATP to prevent EFdA-MP reincorporation, 0.5 μM dTTP, 10 μM ddGTP and 10 mM $MgCl_2$.

Molecular modeling

The sequence of XMRV RT from the VP62 clone was aligned with that of MoMLV RT (PDB: 1RW3) (21,22) using ClustalW. To generate the homology model of XMRV RT, we used the Prime protocol of the Schrödinger software suite (Schrödinger Inc. NY). The resulting molecular model was further energy minimized by OPLS2005 force field using the Impact option of Schrödinger. The final model was validated with PROCHECK v.3.5.4.

RESULTS

Comparison of RT sequences

The XMRV and MoMLV enzymes are closely related (~95% sequence identity) with most of the differences between them being in the RNase H domain (Supplementary Figure S1). While XMRV and MoMLV differ significantly from HIV-1 RT, the known polymerase motifs (A–F) are well conserved in all three enzymes (Supplementary Figure S1). Specifically, the active site aspartates in Motifs A and C (Figure 9) (D150, D224, D225 in XMRV RT; D150, D224, D225 in MoMLV RT; D110, D185, D186 in HIV-1 RT) are conserved in all three RTs. Also, the three enzymes are similar in Motif B, which is involved in dNTP binding and multidrug resistance (AZT and dideoxy-nucleoside drugs) through the decreased incorporation mechanism (27,39–41). Specifically, all three enzymes have a glutamine at the start of this motif (Q151 in HIV-1 RT, Q190 in XMRV RT and Q190 in MoMLV RT). Motif D includes HIV-1 RT residues L210 and T215, which when mutated they enhance excision of AZT from the AZT-terminated primer terminus. This motif is mostly different in XMRV and MoMLV RTs, where the corresponding residues are N226 and A231 (Supplementary Figure S1). K219 of HIV-1 RT Motif D is proximal to

the dNTP-binding pocket and is also conserved in the other enzymes (K235). The DNA primer grip (Motif E) (36,42) in HIV-1 RT ($M_{230}G_{231}Y_{232}$) is slightly different in the gammaretroviral enzymes ($L_{245}G_{246}Y_{247}$). Motif F at the fingers subdomain of all enzymes has two conserved lysines that bind the triphosphate of the dNTP (K65 and K72 in HIV-1 RT; K103 and K110 in XMRV and MoMLV RTs).

Several HIV-1 residues involved in NRTI resistance have the resistance mutations in XMRV and MoMLV RTs (Table 1). Hence, XMRV and MoMLV RTs have a Val as the X residue (codon 223) of the conserved YXDD sequence of Motif C. An M184V mutation at this position in HIV-1 RT causes strong, steric hindrance-based, resistance to 3TC and FTC (43–45), and to a lesser extent to ddI, ABC [reviewed in (46)], and translocation defective RT inhibitors (TDRTIs) (43) (Table 1). Similarly, the M41L mutation, which causes excision-based AZT resistance in HIV is already present in XMRV and MoMLV RT (L81, Table 1). The gammaretroviral enzymes differ from HIV-1 RT in several other HIV drug resistance sites (HIV residues 62, 67, 69, 70, 75, 77, 115, 210, 215) (Table 1). Finally, there are also differences in residues that are essential for NNRTI binding in HIV-1 RT: W229 changes to Y268 in XMRV RT, Y181 to L220, Y188 to L227 and G190 to A229 (Table 1) (27,28,47–49).

Preparation of MoMLV and XMRV RTs

The sequence coding for full-length XMRV RT from the VP-62 clone (NCBI RefSeq: NC_007815) (1) was optimized for expression in bacteria, synthesized by Epoch Biolabs and cloned as described in 'Materials and Methods' section. Both XMRV RT and MoMLV RT were tagged with a hexahistidine sequence at the N-terminus and expressed with a yield of ~2 mg/l of culture. Purified enzymes (>95% pure, Supplementary Figure S2) were stored at −20°C. The presence of NP-40 or glycerol was critical for enzyme stability.

Steady state kinetics of nucleotide incorporation

Initial polymerase activity assays using $T_{d31}/5'$-Cy3-P_{d18a} displayed overall slower polymerase activity of XMRV RT compared to HIV-1 and MoMLV RTs. This observation led us to investigate the steady state nucleotide incorporation properties of XMRV RT using single nucleotide incorporation assays. The estimated values for k_{cat} (19.9 min^{-1} for HIV-1 RT (32), 3.3 min^{-1} for MoMLV RT, 0.6 min^{-1} for XMRV RT) and $K_{m.dNTP}$ (0.07 μM for HIV-1 RT (32), 3.3 μM for MoMLV RT, 3.0 μM for XMRV RT) show that XMRV RT has a drastically reduced efficacy ($k_{cat}/K_{m.dNTP}$) at nucleotide incorporation, compared to both MoMLV and HIV-1 RTs.

DNA binding affinity

To assess if the efficiency of XMRV RT was also affected by a lower DNA binding affinity we measured the DNA binding affinity of the enzymes using three methods: gel-mobility shift assays, pre-steady state kinetics and SPR. Gel-mobility shift assays showed that the $K_{D.DNA}$ for XMRV RT was marginally higher than that for HIV-1 RT and MoMLV RT (data not shown) (50) suggesting weaker binding to DNA.

DNA binding affinity using pre-steady state kinetics

Pre-steady state kinetics allows estimation of the fraction of active polymerase sites as well as the $K_{D.DNA}$ value for the enzyme. The amplitudes of DNA extensions using XMRV RT and/or MoMLV RT at varying DNA concentrations were plotted against the DNA concentration and

Table 1. HIV-1 RT drug resistance mutations with wild-type XMRV RT and MoMLV RT residues

	HIV-1 residue numbers	HIV-1 RT wt	HIV-1 resistance mutations					XMRV RT wt	MoMLV RT wt
			3TC	ABC	TDF	D4T	EFdA		
Thymidine analog mutations (TAMs)	184	M	V	V	–	–	V	V223	V223
	41	M	–	L	L	L	–	L81	L81
	67	D	–	N	N	N	–	G105	G105
	210	L	–	W	W	W	–	N226	N226
	215	T	–	FY	FY	FY	–	A231	A231
	219	K	–			QE	–	K235	K235
Non-thymidine analog regimen mutations	65	K	RN	RN	RN	RN	–	K103	K103
	70	K	EG	EG	EG	–	–	D108	D108
	74	L	–	VI	–	–	–	V112	V112
	75	V	–	TM	M	TM	–	Q113	Q113
	115	Y	–	F	F		–	F155	F155
	69	T	Ins	Ins	Ins	Ins	–	N107	N107
Multi-NRTI resistance mutations	151	Q	M	M	M	M	–	Q190	Q190
	62	A	V	V	V	V	–	P104	P104
	75	V	–	I	–	I	–	Q113	Q113
	77	F	–	L	–	L	–	L115	L115
	116	F	–	Y	–	Y	–	F156	F156
TDRTI Mutations	184	M	V	V	–	–	V	V223	V223
	165	T	–	–	–	–	R	H204	H204

The HIV-1 RT data are based on data from the Stanford HIV Database (85).
wt = wild-type.

the data were fit to the quadratic equation (Equation 2), yielding a $K_{D.DNA}$ of 33 nM for XMRV RT, 19 nM for MoMLV RT (Table 2) and 12.5 nM for HIV-1 RT (32). These values did not change significantly when tested with DNA of different lengths (data not shown). Hence, the transient kinetic experiments confirmed the findings of the gel-mobility shift assays showing XMRV RT to have lower DNA binding affinity than HIV-1 RT.

Binding kinetics of XMRV and HIV-1 RT to double-stranded DNA

Measurements of $K_{D.DNA}$ using gel-mobility shift assays and pre-steady state kinetic methods do not offer insights regarding the kinetics of binding and release of nucleic acid from the viral polymerases. Hence, we used SPR to measure directly DNA binding and the DNA dissociation components of the $K_{D.DNA}$. We attached on the SPR chip a nucleic acid biotinylated at the 5′ template end and immobilized it on a streptavidin sensor chip. Various concentrations of either XMRV or HIV-1 RT were flowed over the chip to measure the association (k_{on}) and dissociation (k_{off}) rates of the enzymes in real time (Figure 1). HIV-1 RT had considerably slower dissociation rates than XMRV RT, and longer dissociation phases were needed to obtain reliable values.

Several methods were tested to best fit our data. The 'heterogeneous ligand' method gave the best fit for both XMRV and HIV-1 RT. In this model the x^2 values for DNA binding to XMRV and HIV-1 RT were 9.3 RU^2 and 48.1 RU^2, respectively, compared to 15.1 RU^2 and 152 RU^2 when we tried fitting the data in a 'homogeneous ligand' model. The former model assumes that RT binds DNA in two different modes and provides two association (k_{on}) and two dissociation constants (k_{off}).

Our data show that XMRV RT has a slightly faster rate of association (k_{on}) than HIV-1 RT. We measured two k_{on} values of $7.3 \times 10^6 M^{-1}s^{-1}$ and $8.2 \times 10^4 M^{-1}s^{-1}$ for XMRV RT versus $7.6 \times 10^5 M^{-1}s^{-1}$ and $1.2 \times 10^6 M^{-1}s^{-1}$ for HIV-1 RT. Interestingly, the dissociation rate of XMRV RT was significantly faster than that of HIV-1 RT ($0.28\,s^{-1}$ and $0.0045\,s^{-1}$ for XMRV RT and 7.8×10^{-4} $s^{-1}$and $0.0076\,s^{-1}$ for HIV-1 RT) (Table 3). This difference in dissociation rate resulted in a $K_{D.DNA}$ at least 1 order of magnitude higher for XMRV RT compared to HIV-1 RT (38 and 54 nM versus 1.0 and 6.1 nM for XMRV and HIV-1 RT, respectively) (Table 3).

Nucleotide binding affinity and optimal incorporation efficiency

A transient-state kinetics approach was used to estimate the dNTP binding affinity ($K_{d.dNTP}$) and maximum nucleotide incorporation rate (k_{pol}) (55). The rates at varying concentrations of next incoming nucleotide (dATP) were determined by plotting the amount of extended primer as a function of time. The rates were then plotted against dATP concentration. The data were fit to a hyperbola (Equation 3). The $K_{d.dNTP}$ for XMRV RT is 26.6 μM and the k_{pol} is $8.9\,s^{-1}$ (Figure 2) (Table 2). Under similar conditions the $K_{d.dNTP}$ and k_{pol} were 1.3 μM and $24.4\,s^{-1}$ for HIV-1 RT (29) and 25 μM and $14.1\,s^{-1}$ for MoMLV RT.

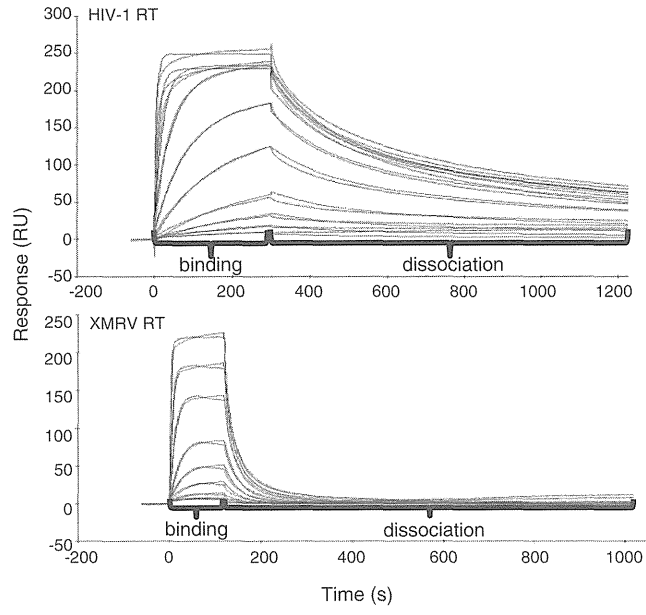

Figure 1. Assessment of $K_{D.DNA}$, k_{on} and k_{off} using surface plasmon resonance. SPR was used to measure the binding affinity of RTs to a nucleic acid substrate. Increasing concentrations of each RT (0.2, 0.5, 1, 2, 5, 10, 20, 50, 100 and 200 nM) were injected over a streptavidin chip with biotinylated double-stranded DNA immobilized on its surface as described in 'Materials and Methods' section. The experimental trace (red) shown is the result of a subtraction of the data obtained from the channel containing the immobilized nucleic acid minus the signal obtained from an empty channel. The black curve represents the fitted data according to the 'heterogeneous ligand' model that assumes two different binding modes for RT on the nucleic acid.

Table 2. Kinetic parameters of DNA binding and synthesis by HIV-1 and XMRV RTs

Nucleotide affinity and incorporation	HIV-1 RT[a]	MoMLV RT	XMRV RT
$K_{d.dNTP}$ (μM)	1.3 ± 0.4	25 ± 5.3	26.6 ± 6.5
k_{pol} (s^{-1})	24.4 ± 0.9	14.1 ± 0.8	8.9 ± 0.6
$k_{pol}/K_{d.dNTP}$ ($s^{-1}\cdot\mu M^{-1}$)	18.8	0.56	0.33
DNA binding affinity:			
$K_{D.DNA}$ (nM)	12.5	19.0	32.5

[a]HIV-1 RT data published previously (29).

Table 3. DNA binding constants for HIV-1 and XMRV RTs from surface plasmon resonance

	HIV-1 RT	XMRV RT
k_{on} ($M^{-1}.s^{-1}$)	7.6×10^5	7.3×10^6
k_{off} (s^{-1})	7.8×10^{-4}	2.8×10^{-1}
$K_{D.DNA1}$ (nM)	1	38 (38-fold)[a]
k_{on} ($M^{-1}.s^{-1}$)	1.2×10^6	8.2×10^4
k_{off} (s^{-1})	7.6×10^{-3}	4.5×10^{-3}
$K_{D.DNA2}$ (nM)	6.1	54 (9-fold)[a]

[a]Increase in $K_{D.DNA}$ (decrease in affinity) with respect to HIV-1 RT. ($K_{D1\text{-}XMRV\ RT}/K_{D1HIV\text{-}1\text{-}RT}$ and $K_{D2\text{-}XMRV\ RT}/K_{D2HIV\text{-}1\text{-}RT}$).

Fidelity of nucleotide incorporation

To assess whether XMRV RT displays high nucleotide incorporation fidelity we monitored the incorporation of three dNTPs by XMRV RT and compared with HIV-1 RT (52). The results of fidelity assay are shown in Figure 3. The lanes marked '4dNTPs' for all enzymes represent the DNA synthesis using a T_{d100}/5′-Cy3-P_{d18a} template-primer in the presence of all four dNTPs. The subsequent lanes, marked '-dNTP', correspond to the synthesis of DNA in the absence of that specific deoxynucleotide triphosphate. The comparison of the DNA synthesis in the absence of one nucleotide by HIV-1 RT, MoMLV RT and XMRV RT shows that HIV-1 and MoMLV RTs were able to misincorporate and extend the primer beyond the missing nucleotide more efficiently than XMRV RT, suggesting that the latter is a less error prone DNA polymerase. It should be noted that the higher fidelity of XMRV is not the result of measuring a smaller number of errors because of the decreased replication rate, as the assay conditions were optimized to allow production of the same amount of full length product in the presence of all four dNTPs for and MoMLV RTs. To further investigate the fidelity of DNA synthesis by XMRV RT, the kinetics of mismatch nucleotide incorporation were carried out in a quantitative manner by monitoring the incorporation of single mismatched nucleotide under pre-steady state conditions. The estimated $K_{D.dTTP}$ (mismatch) and k_{pol} values show that XMRV RT has a lower affinity for a mismatched nucleotide but comparable turnover number than MoMLV RT, suggesting that the observed higher fidelity over MoMLV RT is due to differences during the nucleotide-binding step (Table 4). However, compared to HIV-1 RT, XMRV RT has decreased both affinity and incorporation rate, suggesting that its higher fidelity is the result of both decreased binding of mismatched nucleotides and slow rate of incorporation.

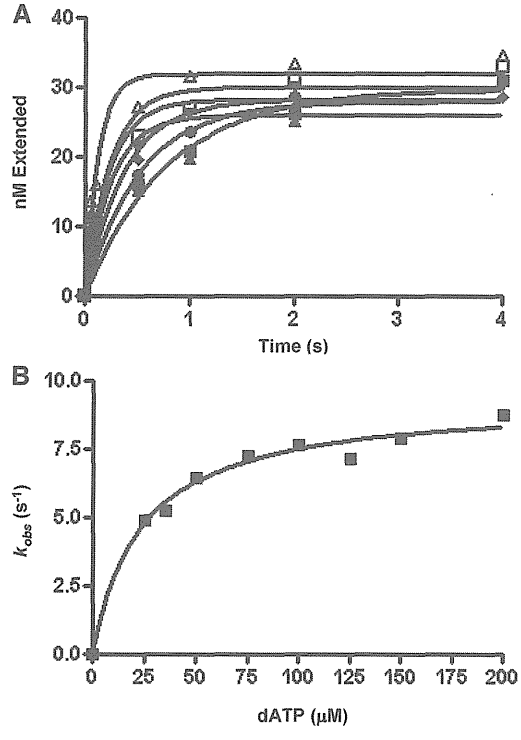

Figure 2. Pre-steady state kinetics of nucleotide incorporation by XMRV RT. 150 nM XMRV RT was pre-incubated with 40 nM T_{d31}/5′-Cy3-P_{d18a} rapidly mixed with a solution containing $MgCl_2$ (5 mM) and varying concentrations of dATP: 25 μM (filled square), 35 μM (filled triangle), 50 μM (filled inverted triangle), 75 μM (filled rhombus), 100 μM (filled circle), 125 μM (open square) and 150 μM (open triangle); and incubated for 0.1 to 6 s before being quenched with EDTA. The DNA product for each dATP concentration was fit to the burst equation (**A**). The burst amplitudes generated for each dATP concentration were then fit to a hyperbola equation (**B**) yielding the optimal rates of dNTP incorporation; k_{pol} ($8.9\,s^{-1}$) and dNTP binding to the RT-DNA complex; $K_{d.dATP}$ (26.6 μM).

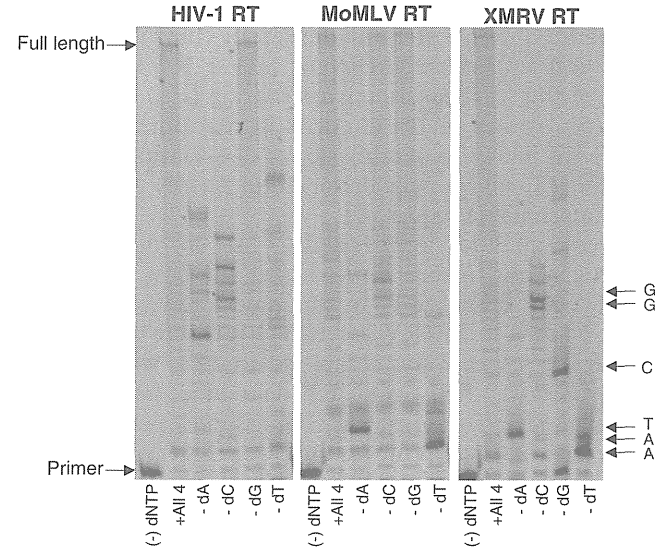

Figure 3. Comparison of *in vitro* fidelity of HIV-1, MoMLV and XMRV RTs. Extension of 10 nM T_{d100}/5′-Cy3-P_{d18a} by HIV-1 RT, MoMLV RT or XMRV RT (20, 50 and 50 nM, respectively) in the presence of 150 μM each of three out of four nucleotides (the missing nucleotide is marked at the bottom of each lane). Reactions were run for 30 min for HIV-1 RT and 45 min for XMRV RT and MoMLV RT. For each enzyme the first lane in each set shows the position of unextended primer, the second lane shows full extension in the presence of all four dNTPs, and each consecutive lane shows extension in the presence of three dNTPs. The arrows on the right mark the expected pauses based on the indicated composition of the template strand.

Table 4. Kinetics of mismatch incorporation for HIV-1, MoMLV and XMRV RTs

Enzyme	HIV-1 RT	MoMLV RT	XMRV RT
$K_{d.dNTP}$ (μM)	9 ± 0.3	38.9 ± 11.6	256 ± 72
k_{pol} (s^{-1})	6.81 ± 1.2	0.16 ± 0.01	0.15 ± 0.018
$k_{pol}/K_{d.dNTP}$ (s^{-1} • μM)	0.756	0.0041	0.00058
Fidelity[a]	0.04	0.007	0.002

[a]Fidelity is the ratio of the incorporation efficiency ($k_{pol}/K_{d.dNTP}$) of the mismatched nucleotide (dTTP) over that of the correct (dATP) ($[k_{pol}/K_d]$dTTP/$[k_{pol}/K_d]$dATP).